Eur Biophys J (1987) 14:441–447

European Biophysics Journal

Neutron scattering by calf lens cytoplasm

A comparison between two models of cataract

D. Laporte[1]* and M. Delaye[2]**

[1] Laboratoire Léon Brillouin, CEN-Saclay, F-91190 Gif-sur-Yvette, France
[2] Laboratoire de Physique des Solides, Bâtiment 510, Université de Paris-Sud, F-91405 Orsay Cedex, France

Received July 7, 1986/Accepted in revised form November 20, 1986

Abstract. Small angle neutron scattering (SANS) was used to compare two models of cataracts: the cold cataract induced in the lens nucleus cytoplasm by lowering the temperature and the opacification induced by calcium in the lens cortex cytoplasm. In both cases opacified cytoplasms display additional scattering at low angles as compared to their clear controls. An analysis of this additional scattering provides quantitative information concerning the size distribution, the number and contrast of the scatterers responsible for lens opacification. The scatterers of cold cataract and of calcium – induced opacification not only have, as shown elsewhere, a different composition but are also found to display completely different sizes (in the thousand Å range for cold-cataract, in the hundred Å range for calcium – induced opacification). These results illustrate the diversity of scatterer types which are able to cause comparable lens opacities.

Key words: Neutron scattering, lens, cataract, calcium, cold cataract

Introduction

Vertebrate eye lenses are made of long fibre cells, enclosing as a major cytoplasmic component lens – specific proteins, the crystallins. α-crystallins (molecular weight 850,000 to 1,100,000) and β-crystallins ($\beta_h \cong 180{,}000$; $\beta_l \cong 60{,}000$) are polydisperse oligomeric proteins, while γ-crystallins are monomers ($\gamma \cong 20{,}000$). Despite the presence in the lens cells of very high crystallin concentrations (200 to 500 mg/ml) (which, a priori, could be expected to scatter an important part of the incident light), the lens is transparent in its normal state. As shown by a previous X-ray study (Delaye and Tardieu 1983), the liquid-like organization of the crystallins inside the lens cytoplasm sufficiently reduces the light scattering to account for this transparency. In contrast, cataracts correspond to an abnormally high scattering of the visible light, the origin of which can be extremely diverse.

In this article we use small angle neutron scattering (SANS) to compare the scatterers responsible for lens opacification in two in-vitro models of cataracts. The first model, the "cold-cataract", is a reversible opacification induced in the nucleus (i.e. the centre) of young mammalian lenses by lowering their temperature. This reversible phenomenon is also observed in isolated cytoplasm. It has been shown to behave like a phase separation (Tanaka and Benedek 1975; Delaye et al. 1981). The demixtion domains, visualized by freeze fracture electron microscopy (Gulik-Krzywicki et al. 1984), contain low molecular weight crystallins, later identified as γ_{IV}-crystallins (Siezen et al. 1985). The second model is an opacification induced by calcium in the cortex (i.e. the periphery) of the lens (Clark et al. 1980; Hightower 1985). This phenomenon, also observed in isolated cytoplasm, has been studied by electron microscopy, which correlated the opacification with the formation of molecular clusters (Delaye et al. 1987).

Light and X-ray scattering have already been applied to both systems (Delaye et al. 1982, 1987) but light wavelengths are too large and X-ray wavelengths too short to provide detailed information on the size distribution of the additional scatterers responsible for lens opacification. In contrast, small angle neutron scattering, filling the gap between X-ray and light scattering, allows a quantitative comparison between the normal lens scattering and the

* The work reported here was begun as a part of the PhD thesis of D. Laporte who died accidentally in September 1984

** To whom offprint requests should be sent

additional scattering associated with lens opacity. The two model systems studied are found to display, at comparable opacification levels, additional scatterers of completely different size. This result illustrates the diversity of biophysical mechanisms leading to lens opacity.

I. Basic scattering equations

We choose to recall these basic equations with the notations used in Zaccai and Jacrot (1983).

The forward coherent intensity scattered by unit volume of an ideal solution of identical globular particles can be expressed as:

$$i\,(c \to 0, q \to 0) = \frac{Mc}{\mathcal{N}} \left(\frac{\partial \varrho_N}{\partial c} \right)^2 , \tag{1}$$

where q is the scattering wavevector, M the molecular weight of the particle, c its concentration in the solution (g/cm^3), $\mathcal{N}$ the Avogadro number, and $\partial \varrho_N / \partial c$ is the neutron scattering length density increment of the solution per unit concentration.

This forward intensity can also be expressed as a function of particle parameters. The density increment $\partial \varrho_N / \partial c$ should then be written as:

$$\frac{\partial \varrho_N}{\partial c} = B - \varrho_N^0 \bar{v} = \frac{\mathcal{N}}{M} \sum (b_i - \varrho_N^0 v_i) , \tag{2}$$

where B is the neutron scattering length per unit mass of the particle, ϱ_N^0 is the neutron scattering length density of the solvent, $\bar{v}$ the specific volume of the particle, b_i refers to the scattering length density in a small volume v_i and the summation $\sum$ bears on the total volume V of one particle. Another formulation is thus:

$$\frac{\partial \varrho_N}{\partial c} = \frac{\mathcal{N}}{M} V \bar{\varrho} \tag{3}$$

with $\bar{\varrho} = \varrho_N - \varrho_N^0$ the contrast between the mean scattering length density of the particle and of the solvent. Combining Eq. (1) and (3) results in:

$$i\,(c \to 0, q \to 0) = \frac{c\mathcal{N}}{M} (V\bar{\varrho})^2 = N (V\bar{\varrho})^2 \tag{4}$$

with N the number of particles per unit volume of the solution.

At finite wavevector q, the intensity $i\,(c \to 0, q)$ scattered by an ideal solution of N identical particles can be written:

$$i\,(c \to 0, q) = N \overline{F(q)^2} = N (V\bar{\varrho})^2 P(q) \tag{5}$$

where $\overline{F(q)^2}$ is the intensity scattered by a single particle, $(V\bar{\varrho})^2$ its limit at $q \to 0$ and $P(q)$ a form factor normalized to 1 at $q = 0$.

When the concentration c is not low enough to make interactions negligible, the scattered intensity $i\,(c, q)$ also involves a structure factor $S\,(c, q)$ describing the spatial correlations (Hansen and McDonald 1976).

$$i\,(c, q) = N \overline{F(q)^2}\, S\,(c, q) . \tag{6}$$

At $c = 0$, $S\,(c, q) = 1$ for any q value. At higher concentrations and in the presence of repulsive interactions $S\,(c, q)$ takes at $q = 0$ a value lower than 1 (the larger c, the lower $S\,(c, 0)$) and then shows damped oscillations around 1.

As shown by previous X-ray experiments (Delaye and Tardieu 1983), the scattering by normal lens cytoplasm, which basically reduces to the scattering of a concentrated crystallin solution, can still be described by a formula analogous to (6) (with modifications taking into account the polydispersity of the solution and the deviations from sphericity of the crystallins).

The forward intensity $i_r(c, q \to 0)$ scattered by transparent lens cytoplasm can than be written as:

$$i_r(c, q \to 0) = \frac{\mathcal{N}}{\bar{M}} (\bar{V}\bar{\varrho}_p)^2\, c\, S_r(c, 0) \tag{7}$$

with $\bar{M}$ the average molecular weight of crystallin proteins, $\bar{V} = \bar{M}\bar{v}/\mathcal{N}$ their average dry volume ($\bar{v}$ is taken as 0.74), ϱ_p the contrast between dry proteic material and water and $c\, S_r(c, 0)$ the factor describing the influence of crystallin concentration on the forward scattered intensity. $\bar{M}$ was determined experimentally as well as $S_r(c, 0)$ for a wide concentration range. In fact for the polydisperse lens cytoplasm, the effective structure factor does not show any oscillation with q but only a progressive increase from $S\,(c, 0)$ towards 1. As a result, the intensity $i_r(c, q)$ displays at high enough c a broad maximum as a function of q, usually called the "interference peak".

The development of cataract is due to the appearance in the cytoplasm of additional scatterers with a contrast with water $\bar{\varrho}_a$ different from that of the bulk cytoplasm $\bar{\varrho}_b$. If these additional scatterers are all made of proteins at concentration c_a while c_b is the protein concentration in bulk cytoplasm then

$$\Delta\varrho_a = \bar{\varrho}_a - \bar{\varrho}_b = \bar{v}\,\bar{\varrho}_p\,(c_a - c_b) = \bar{v}\,\bar{\varrho}_p\,\Delta c_\alpha . \tag{8}$$

For a distribution of additional scatterers the additional scattering $\Delta i\,(q)$ is

$$\Delta i\,(q) = \langle N_a \overline{F_a(q)^2} \rangle = (\bar{v}\,\bar{\varrho}_p)^2 \langle \phi_a V_a \Delta c_a^2 P_a(q) \rangle , \tag{9}$$

where N_a is the number of additional scatterers of species "a" and $\overline{F_a(q)^2}$ their individual scattering, V_a the individual volume of one additional scatterer, $\phi_a = N_a V_a$ the volume fraction occupied by all "a"

scatterers, Δc_a the difference in concentration between species "a" and the bulk and $P_a(q)$ the normalized form factor of scatterer "a". The brackets refer to the average over all species of scatterers. Equation (10) is valid if additional scatterers are scarce enough to avoid spatial correlations ($S_a(c_a, q) = 1 \forall q$) or in the asymptotic regime $q \to \infty$ where the structure factor reaches the value 1. In this limit $q \to \infty$, and if scatterers "a" have a well defined boundary, $\overline{F_a(q)^2}$ satisfies (Porod 1982):

$$\lim_{q \to \infty} q^4 \overline{F_a(q)^2} = 2\pi \Delta\varrho_a^2 A_a \tag{10}$$

with A_a the surface of the additional scatterers. For spherical particles of radius R_a, Eq. (10) is usually satisfied for $q R_a > 4$. Using $A_a = 3 V_a/R_a$ one has in that case:

$$\lim_{q \to \infty} q^4 \Delta i(q) = 6\pi (\bar{v}\,\bar{\varrho}_p)^2 \left\langle \frac{\Delta c_a^2 \phi_a}{R_a} \right\rangle. \tag{11}$$

When visible light is scattered by such structures, additional scattering can be described by a formula analogous to (9). Only the neutron contrast $\Delta\varrho_a$ should be replaced by a contrast for light $\Delta\varrho_a^L$ (Kerker 1969):

$$\Delta\varrho_a^L = (n_a^2 - n_b^2)/(n_a^2 + 2n_b^2) \tag{12}$$

with n_a the refractive index of the additional scatterer and n_b that of bulk cytoplasm. These refractive indices are determined by protein concentrations c_a and c_b. When scatterers are small enough to have a normalized form factor $P(q)$ uniformly equal to 1 over the q range explored by light scattering, their scattered intensity integrated over whole space leads to a turbidity $\Delta\tau$ (Kerker 1969):

$$\Delta\tau = 24\pi^3 (\Delta\varrho_a^L)^2 \langle \phi_a V_a \rangle / \lambda^4, \tag{13}$$

where λ is the wavelength of incident light.

II. Materials and methods

1) *Preparation of the samples*

Nuclear and cortical cytoplasms were separately isolated from fresh calf lenses using the ultracentrifugation procedure described in Clark et al. (1982). Such a procedure eliminates cell membrane fragments while preserving physiological concentrations (i.e. about 0.30 g protein per cm^3 of cortical material and 0.40 g protein per cm^3 of nuclear material). When a different cytoplasmic concentration was required, stock cytoplasm was diluted with a pH 6.8 and 0.15 Eq ionic strength HEPES buffer.

The protein concentration c (g/cm^3) of the samples was evaluated from their refractive index (measured with an Abbe refractometer) and from the experimentally determined relation (Delaye and Gromiec 1983):

$$n = 1.3336 + 0.184\, c\,. \tag{14}$$

Nuclear cytoplasm was simply opacified by lowering its temperature. A transparent nuclear sample as obtained at $T = 18\,^\circ$C was taken as a reference. In cortical cytoplasm opacification was induced by diluting the sample volume $\mathscr{V}$ by a volume $\mathscr{V}/10$ of calcium supplemented buffer so as to obtain 5 to 100 mM Ca final concentration. In this second model, a reference sample was prepared from the same stock, with the same dilution but with no calcium.

2) *Transmittance measurements*

A helium-neon laser beam (Spectra Physics n° 160S) was focused on the samples and the transmitted intensity I was measured on a powermeter (Spectra Physics 404). The relative transmittance Tr was defined as the ratio of the intensity I_t transmitted though 1 cm of the sample under study to the intensity I_r transmitted through the same thickness of reference sample. If the scatterers responsible for cataracts simply result in an additional scattering with respect to the reference sample, then an additional turbidity $\Delta\tau$ (cm^{-1}) can be defined as

$$\mathrm{Tr} = I_t/I_r = \exp(-\Delta\tau)\,. \tag{15}$$

3) *Small angle neutron scattering*

Small angle neutron scattering (SANS) experiments were performed on the PACE apparatus of the ORPHEE reactor (Laboratoire Léon Brillouin – CEN Saclay, France). Lens cytoplasm samples were sealed between two circular quartz plates separated by a 1 mm thick ring. The wavelength of the neutron beam was adjusted at $\lambda = 16$ Å. The accessible wavevector range was then $2.5 \cdot 10^{-3} < q < 2.7 \cdot 10^{-2}$ Å^{-1} (i.e. $230 < 2\pi/q < 2{,}500$ Å) with $\Delta q = 8 \cdot 10^{-4}$ Å^{-1}. Sample holder and background contributions were treated in a standard way and the incoherent scattering (calculated from the scattering of water) was substracted. Neutron scattering measurements were only made with relative units, contrary to previous X-ray measurements which used absolute units (Delaye and Tardieu 1983). In fact using the similarity of the equations for X-ray and neutron scattering and replacing the electronic contrast between protein and water by the corresponding neutron contrast, one can reach, if required, an absolute scale.

III. Results and discussion

1) Transmittance measurements

For both model systems, the onset of opacification was analyzed by transmittance measurements (Fig. 1). Nuclear cytoplasm (Fig. 1 a) is perfectly transparent at 18 °C (reference sample), starts to opacify at 10 °C ($\Delta\tau \cong 0.1\,\mathrm{cm}^{-1}$) and turns opaque at 5 °C ($\Delta\tau \cong 2\,\mathrm{cm}^{-1}$). At 0 °C, the turbidity has further increased to $\Delta\tau \cong 5\,\mathrm{cm}^{-1}$. When the sample is warmed up again, a hysteresis of a few degrees is observed around the phase separation temperature but a perfectly clear sample is recovered at $T = 18$ °C (reference).

In cortical cytoplasm (Fig. 1 b) the opacity is found to develop with calcium molarity and incubation time. After one day incubation at room temperature, $\Delta\tau$ is of the order of $0.05\,\mathrm{cm}^{-1}$ for 5 m*M* calcium, of $0.30\,\mathrm{cm}^{-1}$ for 20 m*M* and of $0.67\,\mathrm{cm}^{-1}$ for 100 m*M*. This range of turbidity is thus comparable to that observed for cold cataract between 11° and 8.5 °C.

2) Small angle neutron scattering (SANS)

a) Reference samples. Figure 2 shows, on a relative scale, the neutron scattered intensities, $i_r(q)$, obtained from the reference samples for both model systems. Both curves display comparable patterns with a marked increase at large q. The main difference is that nuclear cytoplasm scatters about 2 times less than cortical cytoplasm.

These features are in agreement with previous X-ray studies which showed that the organization of the crystallins inside the cytoplasm was liquid like and that low angle data could be simply accounted for by a hard sphere model (Delaye and Tardieu 1983). The increased scattering found for both $i_r(q)$ curves at the large q end corresponds to the rise towards the broad maximum observed in the X-ray intensity curves. This maximum, which results from spatial correlations, was indeed located at $q_m = 2.9 \cdot 10^{-2}\,\text{Å}^{-1}$ for $c = 0.25\,\mathrm{g/cm}^3$ and at $q_m = 4.2 \cdot 10^{-2}\,\text{Å}^{-1}$ for $c = 0.40\,\mathrm{g/cm}^3$. The lower intensity scattered at lower q values by nuclear cytoplasm as compared to cortical cytoplasm results from the stronger spatial correlations in the more concentrated sample. As measured by X-rays, the low q value ($q \ll q_m$) of $c\,S_r(c,q)$ [see Eq. (7)] was indeed found to be about two times smaller for $c = 0.40\,\mathrm{g/cm}^3$ than for $c = 0.25\,\mathrm{g/cm}^3$. The slight increase of $i_r(q)$ found at low q was not expected and might be due to a few membrane fragments left in the cytoplasm during isolation.

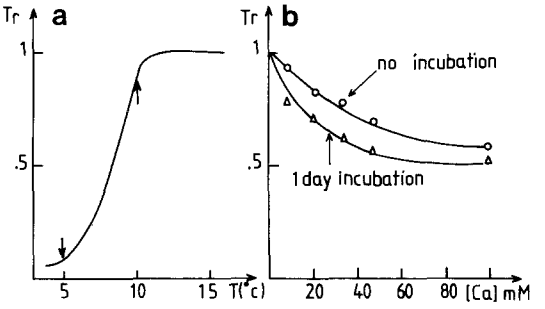

Fig. 1. Evolution of the relative transmittance, Tr, of lens cell cytoplasm in two "models" of cataract. **a** *Cold cataract:* the transmittance Tr of nuclear cytoplasm ($c = 0.40\,\mathrm{g/cm}^3$) is plotted as a function of temperature. The clear cytoplasm ($T = 18$ °C) is taken as a reference; the arrows indicate the conditions analyzed by neutron scattering. **b** *Calcium-induced opacification:* the transmittance Tr of cortical cytoplasm ($c = 0.25\,\mathrm{g/cm}^3$) is plotted as a function of calcium molarity for 2 incubation times (0 and 24 h). A similar sample with no calcium is taken as a reference

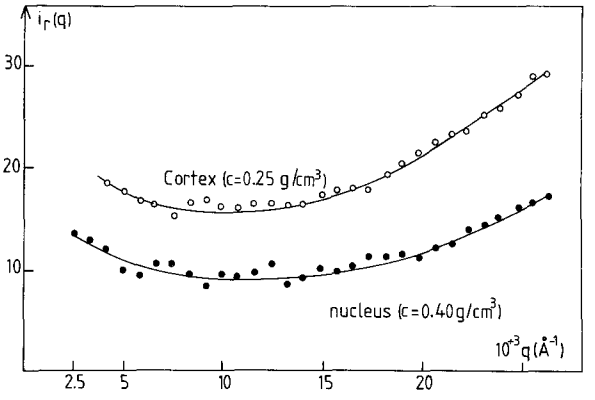

Fig. 2. Small angle neutron scattering intensity, $i_r(q)$, as a function of wavevector q for the two reference samples (cortex (○): $c = 0.26\,\mathrm{g/cm}^3$, 0 m*M* calcium and nucleus (●): $c = 0.40\,\mathrm{g/cm}^3$, $T = 18$ °C)

b) Cold cataract. Neutron scattering $i(q)$ from the nuclear sample at 10 °C and 5 °C was found to be similar to that of the reference for $q > 6 \cdot 10^{-3}\,\text{Å}^{-1}$. This result indicates that in most of the cytoplasm the crystallin organisation is unaffected.

For $q < 6 \cdot 10^{-3}\,\text{Å}^{-1}$ however, an important additional scattering $\Delta i(q) = i(q) - i_r(q)$ was observed, that decreased as a function of q. This scattering, $\Delta i(q)$, is plotted in Fig. 3 on the same scale as in Fig. 2. The inset of Fig. 3 also indicates that $\Delta i(q)$ varies as q^{-4} for $q > 3 \cdot 10^{-3}$. Such behavior suggests that the additional scattering originates from large structures with well defined boundaries [cf. Eq. (10)]. If we approximate these structures to spheres, their radii R_a should satisfy $q R_a > 4$ for $q > 3 \cdot 10^{-3}$ i.e. $R_a > 1{,}300$ Å. If we now suppose that the protein concentration c_a is uniform over the scatterer dis-

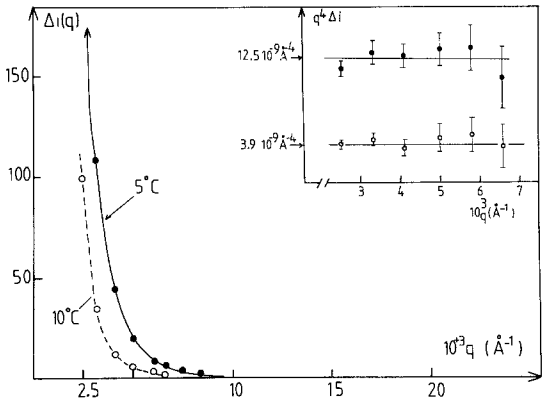

Fig. 3. Additional neutron scattering, $\Delta i(q)$, induced in nuclear cytoplasm by lowering its temperature to 10 °C (○) and 5 °C (●). The inset shows the plots of $q^4 \Delta i$ as a function of q

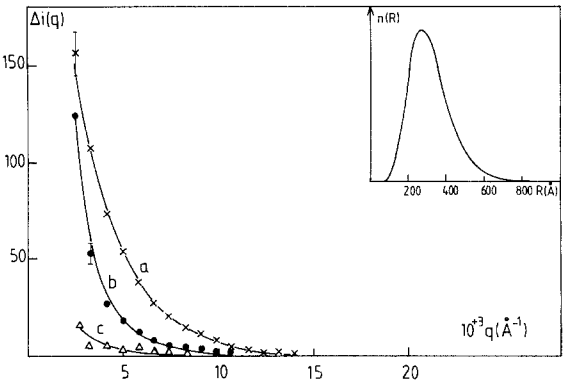

Fig. 4. Additional neutron scattering $\Delta i(q)$ induced by calcium in cortical cytoplasm (*a*) 100 m*M* Ca (×) (*b*) 20 m*M* Ca (●) (*c*) 5 m*M* Ca (△). *Full lines* correspond to scattering simulations $\Delta i(q) \sim \int R^6 P_a(q,R) N(R)\, dR$ using size distributions $N(R) \sim \frac{1}{R} \exp(-(\ln(R/R_0))^2/2\sigma^2)$ (with $R_0 = 280$ Å and $\sigma = 0.35$, 0.5 and 0.40 for (*a*), (*b*) and (*c*) respectively). $P_a(q, R)$ was taken as: $\exp(-q^2R^2/5)$ for $qR < 5$ and as: $\frac{9}{2}(qR)^{-4}$ for $qR > 5$. The *inset* shows the distribution $N(R)$ used to fit curve (*a*) ($R_0 = 280$ Å; $\sigma = 0.45$)

tribution, then Δc is independent of the species "*a*" and Eq. (11) becomes for $q > 4/R_a$

$$q^4 \Delta i(q) = 6\pi (\bar{v}\bar{\varrho}_p \Delta c)^2 \left\langle \frac{\phi_a}{R_a} \right\rangle . \tag{16}$$

Using Eq. (7), the ratio k of this constant $q^4 \Delta i(q)$ over the reference intensity $i_r(c, q)$ for $q \ll q_m$ is equal to

$$k = \frac{[q^4 \Delta i(q)]}{\lim\limits_{q \ll q_m} [i_r(c,q)]} = \frac{6\pi (\Delta c)^2 \mathcal{N}}{\bar{M} c\, S_r(c,0)} \left\langle \frac{\phi_a}{R_a} \right\rangle . \tag{17}$$

At $T = 5$ °C, this ratio is experimentally found to be equal to $12.5 \cdot 10^{-9}/10 = 1.2 \cdot 10^{-9}$ Å$^{-4} = 1.2 \cdot 10^{23}$ cm^{-4}. Using $\bar{M} = 5.6 \cdot 10^5$ daltons and $c\, S_r(c,0) = 10^{-2}$ g/cm^3 for $c = 0.4$ g/cm^3 one deduces that the scatterers responsible for cold cataract satisfy:

$$\Delta c^2 \left\langle \frac{\phi_a}{R_a} \right\rangle \cong 60 \text{ cgs} \quad \text{at} \quad T = 5\,^\circ\text{C} . \tag{18}$$

When analyzed by freeze fracture electron microscopy (Gulik-Krzywicki et al. 1984) the opacified nuclear cytoplasm indeed revealed large globular domains with well defined boundaries, containing densely packed γ-crystallins. At 0 °C, the size histogram $N(R_a)$ of these domains was found to be an asymmetric distribution with R_a ranging from $\cong 1{,}000$ Å to $\cong 1\,\mu$ and showing a maximum around 1,500 Å. The total volume fraction occupied by these domains was estimated to be about $7 \cdot 10^{-2}$.

To identify these domains with the scatterers responsible for lens opacification, one should check that their scattering is compatible with SANS results. The size range observed by those domains is actually compatible with the q^{-4} behavior of $\Delta i(q)$. The various approximations introduced in the above calculation (spherical shape and uniform concentration) seem to be reasonable and Eq. (18) can be used. To estimate $\langle \phi_a/R_a \rangle$ at $T = 0$ °C from the electron microscopy data we attribute the total volume fraction $7 \cdot 10^{-2}$ to the centroid $\bar{R} = 2{,}000$ Å of the distribution $R_a^2 N(R_a)$, which gives $\langle \phi_a/R_a \rangle \sim 3{,}500$ cgs. In fact SANS measurements have not been performed at $T = 0$ °C (turbidity $\tau_a = 5$ cm^{-1}) but at $T = 5$ °C (turbidity $\tau_a = 2$ cm^{-1}). Assuming that Δc does not markedly vary between these two temperatures we still have to estimate the decrease of $\langle \phi_a/R_a \rangle$ (which is an R^2-average in contrast to τ_a which is an R^6-average). Since between 5 and 10 °C, τ_a decreases by a factor 20 (see Sect. III$_1$) and $q^4 \Delta i(q) \approx \langle \phi_a/R_a \rangle$ by a factor $3 \simeq (20)^{1/3}$ we assume that between 0 and 5 °C, $\langle \phi_a/R_a \rangle$ decreases by $(5/2)^{1/3} = 1.35$ i.e. $\langle \phi_a/R_a \rangle \simeq 2{,}600$ cgs at $T = 5$ °C. This leads to $\Delta c \simeq 0.15$ g/cm^3 i.e. to $c_a \simeq 0.55$ g/cm^3. Such a concentration, c_a, indeed appears quite reasonable for densely packed proteins. SANS results and estimations based on FFEM data are thus consistent, which makes the identification between γ-crystallin domains and cold-cataract-scatterers legitimate.

c) Calcium-induced opacification. For cortical samples opacified by calcium one also finds an additional scattering $i(q)$ at low angles, which decreases as a function of q. The difference $i(q)$ is shown in Fig. 4 (same intensity scale as in Figs. 2 and 3) for cortical samples incubated for 2 to 4 days at room temperature with 5, 20 and 100 m*M* calcium respectively. Figure 4 shows that higher calcium molarities enhance the additional scattering. As compared to Fig. 3, $\Delta i(q)$ spreads over a much larger q-range. Indeed the $\Delta i(q)$ values measured for 100 m*M*

calcium can be correctly fitted (full line) by the size distribution shown in the Fig. 4 inset (log-gaussian distribution (Kerker 1969):

$$N(R) \sim 1/R \exp(-(\ln(R/R_0))^2/2\sigma^2)$$

with $R_0 = 280$ Å and $\sigma = 0.35$). Of course the size distribution of the Fig. 4 inset is not a unique fit to the SANS data but it provides an estimate of the mean size, variance and asymmetry of the scatterer distribution. The curve found for 20 and 5 mM calcium can be satisfactorily fitted with similar size distributions ($R_0 = 280$ Å; $\sigma = 0.5$ for 20 mM and $R_0 = 280$ Å; $\sigma = 0.4$ for 5 mM). Let us assume that the scatterers are scarce enough to scatter independently and that their internal protein concentration c_a is independent of their size. Their scattering $\Delta i(q)$ can then be written using Eq. (9):

$$\Delta i(q) = (\bar{v}\,\bar{\varrho}_p\,\Delta c)^2 \langle \phi_a V_a P_a(q) \rangle . \tag{19}$$

The ratio $h(q)$ between $\Delta i(q)$ and the reference intensity $\lim_{q \ll q_m} i_r(c, q)$ (Eq. (7)) is thus:

$$h(q) = \Delta i(q) / \lim_{q \ll q_m} i_r(c, q) = \frac{\mathcal{N}(\Delta c)^2 \langle \phi_a V_a P_a(q) \rangle}{\bar{M} c\, S_r(c, 0} \tag{20}$$

At $q_1 = 3.3 \cdot 10^{-3}$ Å^{-1}, $h(q_1) = 6.9$ for 100 mM Ca (see Figs. 2 and 4). Using the values $\bar{M} = 5.6 \cdot 10^5$ daltons and $c\,S_r(c, 0) = 2 \cdot 10^{-2}$ g/cm^3 at $c = 0.25$ g/cm^3 (Delaye and Tardieu 1983), we find that calcium induced scatterers satisfy:

$$\Delta c^2 \langle \phi_a V_a P_a(q_1) \rangle = 1.3 \cdot 10^{-19} \text{ cgs} \quad \text{for}$$
$$q_1 = 3.3 \cdot 10^{-3} \text{ Å}^{-1} \quad \text{and} \quad 100 \text{ m}M \text{ Ca}. \tag{21}$$

With the histogram $N(R_a)$ shown in the Fig. 4 inset the distribution $g(R_a) = \phi(R_a)\, V(R_a)\, P(R_a, q_1) \simeq R_a^6 N(R_a)\, P(R_a, q_1)$ displays for $q_1 = 3.3 \cdot 10^{-3}$ Å^{-1} a centroid around $\bar{R} = 500$ Å $= 5 \cdot 10^{-6}$ cm.

When analyzed by freeze fracture electron microscopy (Delaye et al. 1987), calcium opacified cytoplasm shows additional structures as compared to normal cytoplasm, which appear as small globular clusters of molecules. For 1 day incubation at 100 mM Ca, the size histogram of these clusters displays a maximum around $R = 220$ Å and extends above $R = 500$ Å. The total volume fraction occupied by these structures is of the order of $6 \cdot 10^{-3}$.

The size histogram found in the FFEM study agrees with that extracted from the SANS study (Fig. 4 inset). To be able to identify FFEM clusters with calcium-induced scatterers, it is now necessary to check that the intensity that they scatter is compatible with that measured by SANS, in other words that Eq. (20) is satisfied. The FFEM clusters are indeed scarce enough to consider them as independent scatterers. Let us approximate $\langle \phi_a V_a P_a(q_1) \rangle$ by attributing the total volume fraction $6 \cdot 10^{-3}$ to $\bar{R} = 500$ Å (i.e. $V_a \simeq 5 \cdot 10^{-16}$ cm^3, $P_a(q_1, \bar{R}) \simeq 0{,}6$). To satisfy Eq. (20) one then requires a concentration difference $\Delta c \simeq 0.27$ g/cm^3 i.e. an internal protein concentration $c_a \simeq 0.52$ g/cm^3 for the molecular clusters. Such a concentration is quite reasonable for a dense packing of globular subunits. Since these calcium induced clusters (in contrast to cold cataract domains) are small enough to validate Eq. (13), the corresponding turbidity can be evaluated as $\Delta\tau = 0.23$ cm^{-1} with $\lambda \simeq 5 \cdot 10^{-5}$ cm, $n_a = 1.433$ and $n_b = 1.380$ (cf. Eq. (14)). This turbidity corresponds to a transmittance $T_r = 0.79$ while the measured one was 0.5. Considering the number of approximations involved in the calculations the agreement is quite satisfactory and calcium-induced clusters can be legitimately considered as the scatterers responsible for the opacification.

IV. Conclusion

In both models of lens opacification additional neutron scattering was detected at low angles in the turbid samples as compared to their clear reference. Quantitative information could be drawn from these SANS experiments concerning the sizes, contrast and volume fraction of the additional scatterers responsible for lens opacification. While light wavelengths were too large and X-ray wavelengths too short to correctly estimate the size of those scatterers, neutron scattering appears to be well suited to distinguishing between the scatterers of cold cataract (in the thousand Å range) and those induced by calcium (in the hundred Å range).

Small angle neutron scattering also complements previous electron microscopy studies by demonstrating that the additional structures visualized in the micrographs can be identified with the scatterers responsible for lens opacification. Such a comparison between the scattering of structures suspected to cause lens opacification and direct scattering measurements is an essential step in cataract mechanism studies, which is too often omitted.

Finally, this study illustrates the diversity of cataract mechanisms. It shows that comparable opacities may originate from light scatterers with not only different composition but also different sizes and different contrasts.

Acknowledgements. We thank J. Teixeira for his assistance in SANS experiments and A. Tardieu for critical reading of the manuscript. This work was pursued under a MIR grant (interface Physique Biologie) and an INSERM grant (contrat de recherche externe financé par la CNAMTS).

References

Clark JI, Mengel L, Bagg A, Benedek GB (1980) Cortical opacity, calcium concentration and fibre membrane structure in the calf lens. Exp Eye Res 31:399–410

Clark JI, Delaye M, Hammer P, Mengel L (1982) Preparation and characterization of native lens cell cytoplasm. Curr Eye Res 1:695–704

Delaye M, Gromiec A (1983) Mutual diffusion of crystallin proteins at finite concentrations: a light scattering study. Biopolymers 22:1203–1221

Delaye M, Tardieu A (1983) Short range order of the crystallin proteins accounts for eye lens transparency. Nature 302:415–417

Delaye M, Clark JI, Benedek GB (1981) Coexistence curves for phase separation in the calf lens cytoplasm. Biochem Biophys Res Commun 100:908–914

Delaye M, Clark JI, Benedek GB (1982) Identification of the scattering elements responsible for lens opacification in cold cataracts. Biophys J 37:647–656

Delaye M, Danford E, Clark JI, Krop B, Gulik-Krzywicki T, Tardieu A (1987) Effect of calcium on the calf lens cytoplasm. Exp Eye Res (in press)

Gulik-Krzywicki T, Tardieu A, Delaye M (1984) Spatial reorganization of low-molecular weight proteins during cold cataract opacification. Biochim Biophys Acta 800: 28–32

Hansen JP, McDonald IW (1976) Theory of simple liquids. Academic Press, New York

Hightower KR (1985) Cytotoxic effects of internal calcium on lens physiology: a review. Curr Eye Res 4: 453–459

Kerker M (1969) The scattering of light and other electromagnetic radiation. Academic Press, New York

Porod G (1982) In: Glatter O, Kratky O (eds) Small angle X-ray scattering. Academic Press, New York, pp 17–51

Siezen RJ, Fisch MR, Slingsby C, Benedek GB (1985) Opacification of γ-crystallin solutions from calf lens in relation to cold cataract formation. PNAS 82:1701–1705

Tanaka T, Benedek GB (1975) Observation of protein diffusivity in intact human and bovine lenses with application to cataract. Invest Ophtalmol 14:449–456

Zaccai J, Jacrot B (1983) Small angle neutron scattering. Ann Rev Biophys Bioeng 12:139–157